Geophysical Research Letters

RESEARCH LETTER
10.1029/2025GL120498

Estimating Ice Cover on the Great Lakes Using Seismic Ambient Noise

Joshua B. Russell[1] and **Christopher J. W. Carchedi**[2]

[1]Department of Earth and Environmental Sciences, Syracuse University, Syracuse, NY, USA, [2]Earth and Planets Laboratory, Carnegie Science, Washington, DC, USA

Key Points:

- Great Lakes microseism noise (0.5–2 Hz) observed on nearby seismometers decreases linearly with increasing ice cover
- A linear transfer function is empirically determined and used to estimate daily lake ice cover from seismic noise with reasonable accuracy
- Seismic noise can reliably track lake ice cover offering new possibilities for monitoring lakes in remote regions

Supporting Information:

Supporting Information may be found in the online version of this article.

Correspondence to:

J. B. Russell,
jbrussel@syr.edu

Citation:

Russell, J. B., & Carchedi, C. J. W. (2026). Estimating ice cover on the Great Lakes using seismic ambient noise. *Geophysical Research Letters*, *53*, e2025GL120498. https://doi.org/10.1029/2025GL120498

Received 7 NOV 2025
Accepted 16 FEB 2026

Author Contributions:

Conceptualization: Joshua B. Russell
Data curation: Joshua B. Russell, Christopher J. W. Carchedi
Formal analysis: Joshua B. Russell, Christopher J. W. Carchedi
Funding acquisition: Joshua B. Russell
Investigation: Joshua B. Russell, Christopher J. W. Carchedi
Methodology: Joshua B. Russell, Christopher J. W. Carchedi
Project administration: Joshua B. Russell
Resources: Joshua B. Russell
Software: Joshua B. Russell, Christopher J. W. Carchedi
Supervision: Joshua B. Russell
Validation: Joshua B. Russell
Visualization: Joshua B. Russell, Christopher J. W. Carchedi

Abstract Lake ice impacts seismic noise on nearby seismometers, and therefore seismic observations can be used to monitor ice changes. However, the transfer function describing how lake-microseism noise covaries with ice cover has not been quantified. We use seismic data from a long-operating station near Lake Superior and satellite-derived lake ice cover from 2009 to 2024 to determine their covariance. A linear model calibrated using annual ice cover averaged during the coldest months (15 February–9 March) explains ∼87% of the variance in 0.5–2 Hz seismic noise averaged during the same period. This 15-year-calibrated model is used to predict daily ice cover during the 2014 Polar Vortex with reasonable accuracy, explaining ∼58% variance in the daily 0.5–2 Hz noise. One season of daily lake ice cover data is sufficient to calibrate the model. During unfrozen periods, 0.25–0.5 Hz lake-wave power explains ∼75% of the variance in the daily averaged 0.5–1 Hz seismic noise, consistent with the secondary microseism mechanism.

Plain Language Summary The warming climate has led to increased ice loss across the planet. In winter 2023–2024, average ice cover on the Great Lakes was <10%, the lowest in recorded history by the NOAA Great Lakes Environmental Research Laboratory. Seismometers are sensitive to the vibrations caused by lake waves interacting with the lake bed and coastlines, and because presence of lake ice reduces wave action, frozen periods lead to quieter seismic conditions. In this study, we show that seismic data can therefore be used to predict ice cover with reasonable accuracy by tuning a simple linear model. This model can explain about 87% of the yearly variations in seismic noise averaged during the coldest months and is able to accurately estimate daily ice cover during the extreme winter of the 2014 Polar Vortex (explaining ∼58% of the daily noise variance). During unfrozen periods, we are able to use seismic data to match wave buoy spectral data on the lake. Overall, this work shows that seismic data can provide a reliable way to track lake ice and wave activity, offering new possibilities for monitoring lakes in remote regions where such estimates do not currently exist.

1. Introduction

A changing climate has contributed to faster rates of ice loss from lakes across the Northern Hemisphere (Imrit & Sharma, 2021). The Great Lakes are of particular importance because they are some of the largest freshwater lakes in the world, play an important role in local weather (Wang et al., 2022), and have economic significance tied to the St. Lawrence Seaway connection to the Atlantic Ocean. In winter 2024, average ice cover on the Great Lakes was <10%, the lowest ever recorded by the Great Lakes Environmental Research Laboratory (GLERL) of the National Oceanic and Atmospheric Administration (NOAA) since 1973. Here, "winter 2024" refers to the 2023–2024 winter season and is the convention used throughout this work. This vast GLERL database of lake ice cover shows long-term trends in ice coverage but lacks the temporal resolution needed to understand wave-ice interactions at shorter time and length scales. In addition, uncertainties are typically not reported by modern ice cover data products and may evolve over time with new monitoring technologies. Seismic observations offer complementary information that can illuminate processes occurring at shorter time scales and in remote locations (e.g., Maurer et al., 2020).

Lakes of various size have been shown to produce a microseism signal in a frequency band of ∼0.5–2 Hz due to wave action, which can be detected by seismometers within ∼100 km of the lake (Anthony et al., 2018, 2022; Carchedi et al., 2022; Farrell et al., 2023; Smalls et al., 2019; Xu et al., 2017). The magnitude of lake-generated microseism noise is noticeably reduced when lakes freeze due to suppression of wave action, as demonstrated at Yellowstone Lake (Xu et al., 2017) and the Great Lakes (Anthony et al., 2018). A similar connection between sea ice and 0.5–2 Hz seismic noise was first documented at stations in Alaska along the Bering Sea coast (Tsai &

Writing – original draft: Joshua B. Russell, Christopher J. W. Carchedi
Writing – review & editing: Joshua B. Russell, Christopher J. W. Carchedi

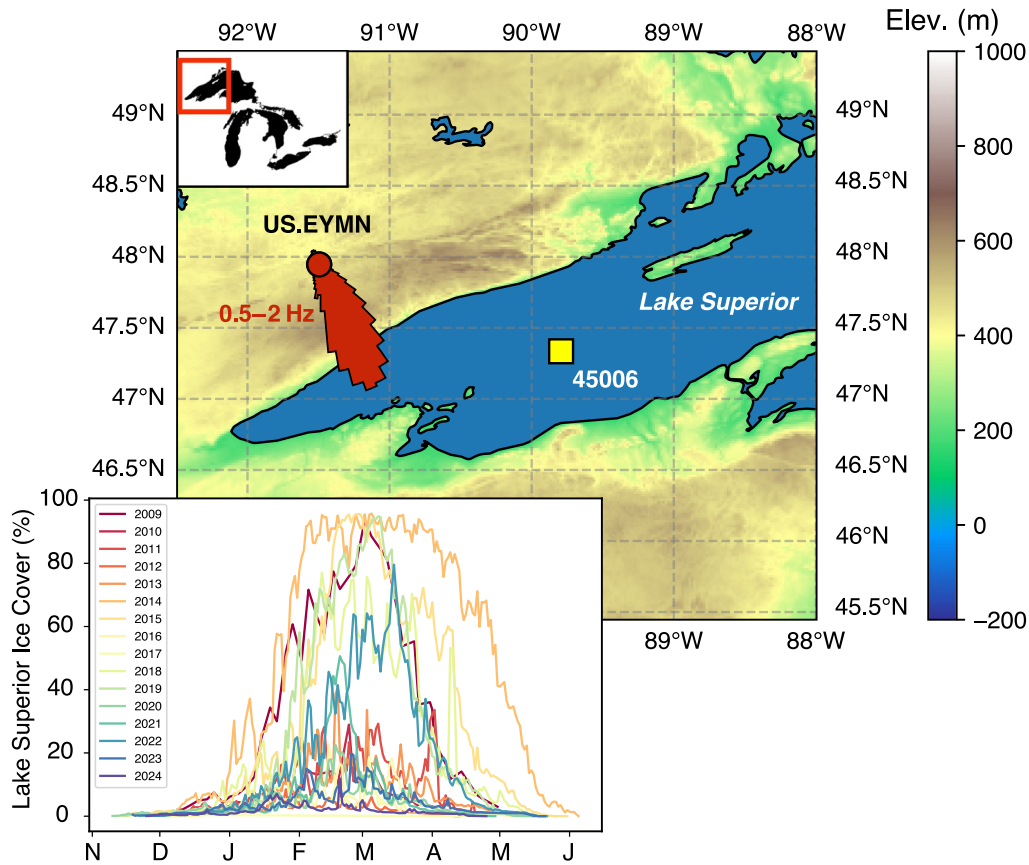

Figure 1. Map of the study region showing the locations of seismic station EYMN (red circle) and buoy 45006 (yellow square). Station EYMN is located ~60 km from Lake Superior. Rayleigh wave arrival angles resulting from noise polarization analysis of data from 2018 for 0.5–2 Hz (red polar histogram) indicate Rayleigh waves arriving from the southeast, in the direction of the nearest lake shore. The inset map shows average daily Lake Superior ice cover in the winter months from 2009 to 2024 estimated from satellite imagery by the Great Lakes Environmental Research Laboratory.

McNamara, 2011), and it has been shown that a simple linear model can be used to describe the influence of sea ice on seismic power (Chen et al., 2025; John & West, 2025b; Tsai & McNamara, 2011). Therefore, lake-generated noise observed at seismic stations may be used to remotely monitor ice conditions on nearby lakes. As average ice cover has been decreasing on the Great Lakes since 1973, conditions are expected to be noisier in the 0.5–2 Hz band during winter months on average, potentially making detections of small earthquakes more challenging in the region. Despite the importance of changing ice conditions on the lakes, the transfer function between lake ice cover and seismic noise has not yet been quantified.

The Great Lakes are especially well suited for studying the relationship between lake ice, lake wave action, and seismic noise. In addition to having the well maintained high-quality GLERL ice cover data product, the Great Lakes are well instrumented by broadband seismic stations operated by the US Geological Survey (USGS) as well as wave buoys that record hourly lake conditions (Figure 1). Combined, these data sets describe the relationships between lake-generated microseism noise and lake conditions. The underlying mechanism that produces the lake-generated microseism in the Great Lakes during unfrozen periods is still uncertain and may differ from that of conventional ocean microseisms (Anthony et al., 2018).

The primary motivation of this study is to determine the degree of correlation between lake-generated microseism and lake ice cover on the Great Lakes and to construct a transfer function between the two that allows seismic prediction of ice cover. We show that lake ice cover and seismic noise covary linearly, providing a simple relationship for estimating ice cover from seismic data. The model is then applied to seismic data to successfully reconstruct daily ice cover on Lake Superior during the 2014 "Polar Vortex" winter season.

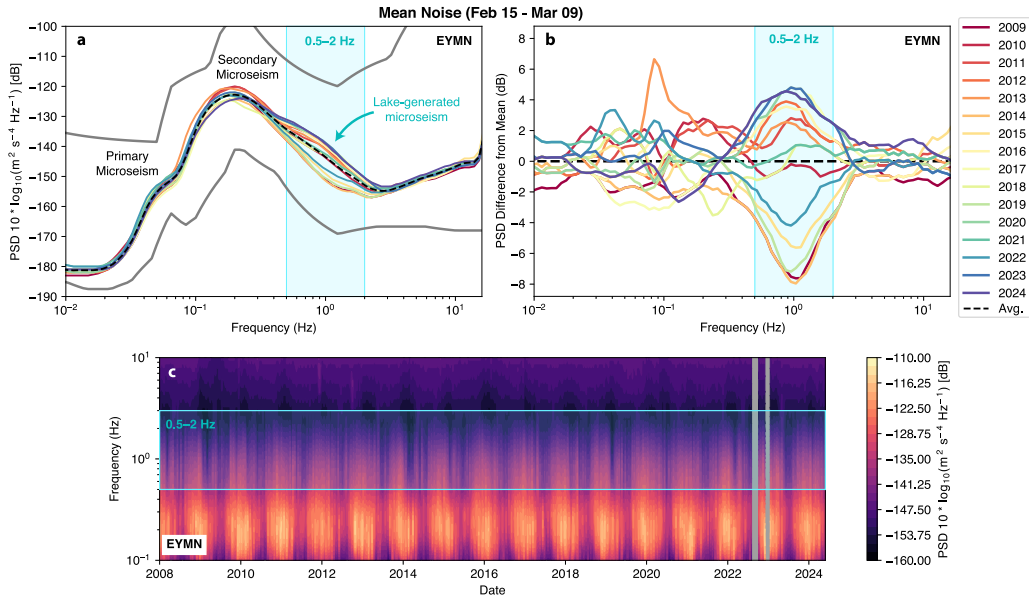

Figure 2. Vertical component (BHZ) power spectral densities (PSDs) for station EYMN from 2009 to 2024. (a) Annual median PSDs during 15 February–9 March, approximately during peak ice conditions. The mean PSD across all years is shown by the black dashed line. The lake-generated microseism from 0.5 to 2 Hz is indicated by the blue shaded region. (b) PSDs with the mean subtracted to highlight deviations from average. Note the large ∼10 dB variation in noise within the lake-generated microseism band. (c) Spectrogram showing the annual variations in noise from 0.1 to 10 Hz constructed from an 8-day moving median.

Although we focus here on Lake Superior, in Supporting Information S1 we show additional ice cover results for a station located near Lake Erie (Figure S2 in Supporting Information S1) and another located between Lakes Huron and Ontario (Figure S3 in Supporting Information S1). Most lakes around the world do not have such high-quality estimates of lake ice cover because they are too remote and/or too small to accurately estimate ice cover using current satellite-based techniques. Our study establishes a simple framework that is a first step toward remotely monitoring lake ice conditions in such locations.

2. Data and Methods

2.1. Seismic Data

We use seismic data from 2009 to 2024 from station EYMN operated by the USGS since 1994 and located near the westernmost tip of Lake Superior in Ely, MN (Figure 2). We use vertical component (BHZ) 40 Hz sample rate data. This broadband station has operated continuously with few data gaps and has low levels of anthropogenic noise. As it is located on the western edge of Lake Superior, it is also isolated from the influence of the other Great Lakes in the region.

Probability density functions (PDFs) of power spectral density (PSD) are queried from EarthScope's Modular Utility for Statistical Knowledge Gathering (MUSTANG) system (Casey et al., 2018), enabling efficient extraction of large volumes of spectral data. We obtain PSD estimates from the median of the PDF within a desired time window (Russell, 2026). The MUSTANG PSDs are precalculated via McNamara and Buland (2004), which employs liberal smoothing. John and West (2025a, 2025b) demonstrate that these smoothed PSDs are appropriate for obtaining accurate seismic power estimates when averaged over a finite band of frequencies.

As expected, we observe the strongest noise and largest seasonal variability in the 0.1–0.5 Hz band (Figure 2c), corresponding to the oceanic secondary microseism (e.g., Janiszewski et al., 2022). It is caused by ocean swells of similar frequency traveling in opposite directions generating standing wave pressure fluctuations at the seafloor at twice the swell frequency (Ardhuin et al., 2011, 2015; Longuet-Higgins, 1950). Because this process produces Rayleigh waves at twice the frequency of the swell, it is often referred to as the "double-frequency" mechanism

for microseism generation. We observe that the secondary microseism is strongest in winter months, which is due to larger storm-generated ocean swells during those months (Ardhuin et al., 2012).

For PSDs averaged within the coldest months annually (15 February–9 March), we find the largest year-to-year variability within the 0.5–2 Hz lake-generated microseism band (Figures 2a and 2b). Within this band, we observe a ∼10 dB variation in power between 2014 (the Polar Vortex, high ice cover) and 2024 (low ice cover). This signal is the primary target of this study.

2.2. Rayleigh Wave Polarization Analysis

In addition to lake-generated microseism, 0.5–2 Hz seismic noise may originate from sources such as ocean waves at the coastline (John & West, 2025b; Tsai & McNamara, 2011) or anthropogenic noise. Due to seismic attenuation, noise sources within ∼100 km of the station likely dominate the PSDs at 0.5–2 Hz (Tsai & McNamara, 2011).

To demonstrate that the large variations in 0.5–2 Hz noise that we observe are due to surface waves from the lake-generated microseism, we perform a Rayleigh wave polarization analysis at EYMN within this band for year 2018 following Park et al. (1987) and Koper and Hawley (2010) (Figure 1). Details of this analysis are summarized in Supporting Information S1, and the methods are described in more detail in the Appendix of Carchedi et al. (2022). The resulting arrival angles in Figure 1 show that Rayleigh wave energy in the 0.5–2 Hz band is dominantly arriving from the southeast (∼150° azimuth), in the direction of the nearest lake shore. No seasonal or diurnal variation is found (Figure S5 in Supporting Information S1), supporting that the lake-generated microseism is consistently the strongest signal in this frequency band.

2.3. Ice Cover Data

We obtain lake-averaged daily estimates of percent ice cover on Lake Superior from 2009 to 2024 from the Great Lakes Ice Cover (GLIC) data set. This data set is jointly maintained by the US National Ice Center (USNIC) and Canadian Ice Service (CIS) and provides estimates of ice cover for each of the Great Lakes at 18:00 UTC daily. This lake-wide daily average ice cover value is a spatial average of daily gridded data (∼1.8 km resolution) (Yang et al., 2020) calculated and reported by the GLERL (see Data Availability Statement). The gridded data product is constructed from a combination of synthetic aperture radar (SAR), visible and infrared imagery, and meteorological data and extends back to 1973 (Simard et al., 2005). From 1973 to 2007, temporal and spatial resolution of reported ice cover varied and was later interpolated to the modern resolution (24 hr, 1.8 km) by Yang et al. (2020). We therefore focus on ice cover data after 2007 reported at the modern resolution to avoid processing artifacts. Typical spatial distributions of ice cover for Lake Superior are shown in Figure S7 in Supporting Information S1. Ice tends to begin forming at the lake edges and freezes inward toward the lake interior where bathymetry is typically deepest.

These lake ice observations show that ice cover typically peaks between February and April (Figure 1). The season with highest ice cover in the data set is 2014 and the lowest is 2024. In order to compare ice cover observations with seismic PSDs, we similarly average ice cover between 15 February and 9 March each year (Figure 3). When considering daily ice cover in Section 3.2, we use the unmodified GLIC daily estimates.

2.4. Wave Buoy Data

Wave buoys provide an incredible wealth of data including both meteorological (wind speed, air temperature, sea temperature, and peak wind) and swell data (significant wave height, spectral wave density, and direction). Here, we use spectral wave density, which has a clear theoretical connection to wave state (e.g., Ardhuin et al., 2012) and allows for isolation of dominant wave periods of interest. Useful information may also be gleaned from simpler components of the data set, such as significant wave height (Anthony et al., 2018; Farrell et al., 2023; John & West, 2025b), which correlates with maximum spectral wave density but lacks frequency information.

We use data from wave buoy 45006 (Figure 1) operated by the National Data Buoy Center and located ∼145 km from EYMN and ∼75 km from the nearest shoreline. This is the nearest open-water wave buoy to seismic station EYMN. We extract data from its 2013 operating period: 27 March–23 September. Wave buoys on the Great Lakes operate only during unfrozen periods (March–November, on average). They are also limited in bandwidth

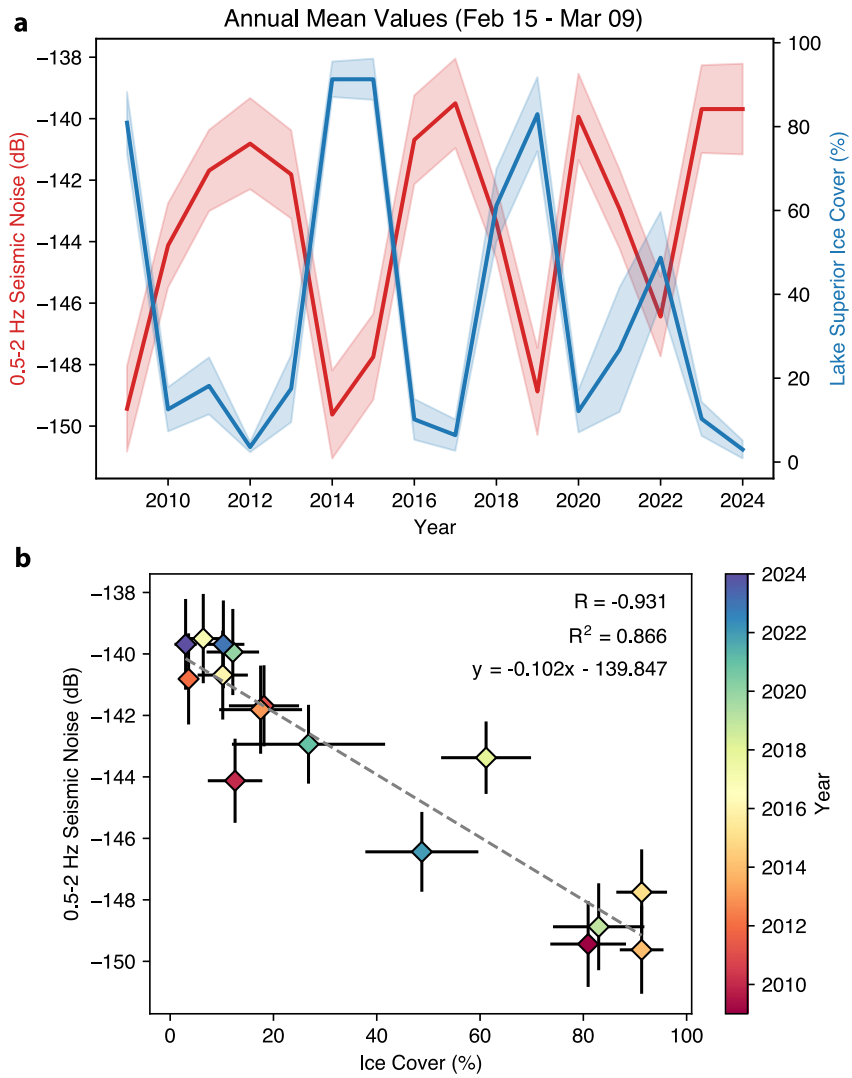

Figure 3. Correlation between 0.5–2 Hz seismic noise measured at EYMN and ice cover on Lake Superior during 15 February–9 March. (a) Power spectral densities from Figure 2 averaged in the 0.5–2 Hz band are shown in red. Mean (15 February–9 March) lake ice cover on Lake Superior estimated from satellite data is shown in blue. Shading indicates 1 standard deviation. (b) Linear correlation between the two quantities shown in panel (a). Color of each symbol indicates year as in previous figures and bars show 1 standard deviation. The gray dashed line shows the best fit linear model. Changes in ice cover explain ~87% of the variance observed in average seismic noise.

compared to seismic observations due to having a sample rate of 1 Hz, meaning they record lake wave frequencies only up to ~0.5 Hz.

3. Results

3.1. Correlation Between Averaged Yearly Lake Ice and Seismic Power

A strong negative correlation is observed between the yearly 0.5–2 Hz seismic noise averaged between 15 February and 9 March from 2009 to 2024 and yearly ice cover on Lake Superior averaged during that same time period (Figure 3). Furthermore, we find a slight overall increase in average seismic noise over time associated with the overall reduction in average ice cover.

A linear model explains the yearly data with a high correlation coefficient of $R = -0.93$, meaning that changes in average ice cover explain ~87% of variance in the average seismic observations. We chose to average over 15 February–9 March in order to capture the portions of the season with the highest potential for ice cover and thus,

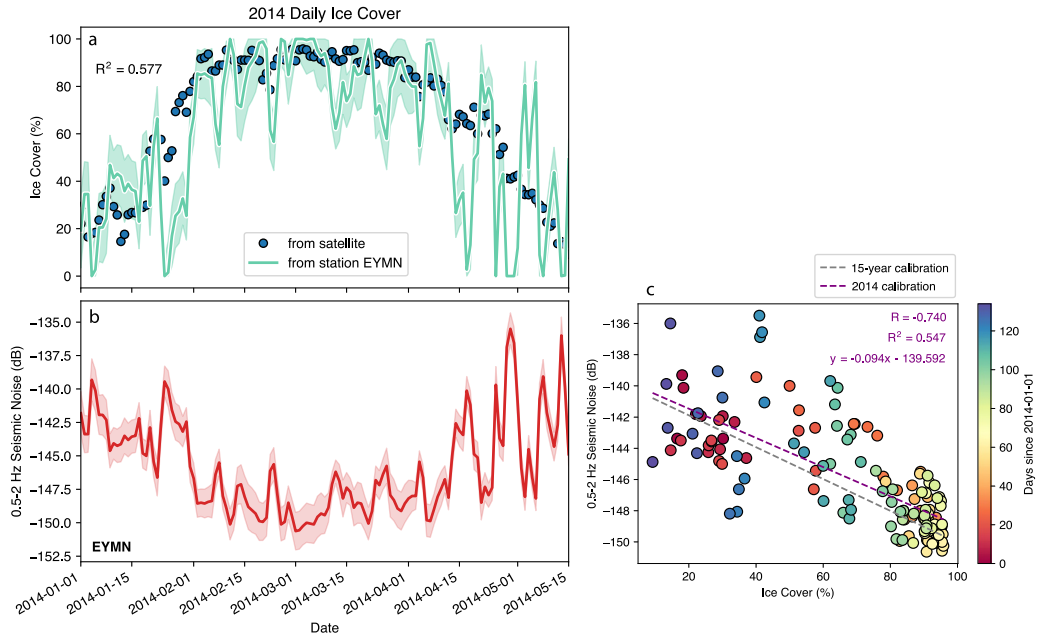

Figure 4. Application of the linear model to estimate daily ice cover from seismic noise observations in 2014. (a) Daily ice cover from 1 January to 15 May 2014 directly predicted from seismic data at station EYMN. The linear model from Figure 3 calibrated from 2009 to 2024 is used in the prediction. Satellite observations are shown by the blue circles and the prediction from 0.5 to 2 Hz seismic data is shown in green. (b) Seismic power spectral density (PSD) observations in the 0.5–2 Hz band at station EYMN used for the predictions in panel (a). Seismic noise estimates are the 8-day moving median PSD averaged within the 0.5–2 Hz band, and shading indicates 1 standard deviation. (c) Data correlations comparing the 15-year calibrated model (gray) from Figure 3 used for (a) with a model calibrated on the data from 2014 (purple). The two models are comparable within the data scatter, demonstrating that one season of ice cover data is sufficient to calibrate the model.

the largest range in ice cover values over all 15 years. This averaging should also reduce the influence of short-timescale variations in lake wave state (e.g., due to daily variations in wind speed) or local transient noise sources near the seismometer, better isolating the impact of ice cover on seismic noise.

Similar relationships are found for seismic stations located near Lake Erie and Lake Huron/Ontario, which are included in Figures S2 and S3 in Supporting Information S1. The model parameters differ for other lake-station pairings due to physical factors that are discussed in further detail in Section 4. This high level of correlation demonstrates promise for using seismic observations to monitor ice cover on nearby lakes.

3.2. Daily Seismic Estimation of Lake Ice Cover

With the well-calibrated model from averaged yearly data from 2009 to 2024 (Figure 3), we seek to test its predictive power at daily timescales. Daily estimates of ice cover from seismic noise are compared to the satellite-derived GLIC estimates from 1 January to 15 May 2014 in Figure 4. This time period captures a northeastern "Polar Vortex," which produced the highest ice cover on the Great Lakes to date, leading to a strong reduction in seismic noise (Anthony et al., 2018).

We find significant correlation between daily lake-generated noise and daily lake ice cover (albeit less strong, as expected). Daily ice cover accounts for ~58% of variance ($R = -0.74$) in the 0.5–2 Hz lake-generated seismic noise. We also re-calculate coefficients for the linear model using only the 2014 daily ice cover and 0.5–2 Hz daily noise at EYMN to compare with the 15-year calibrated model from Section 3.1. We find that the linear model constructed using only the 2014 daily data is comparable to the 15-year calibrated model, both plotting well within the data scatter (Figure 4c and Figure S4 in Supporting Information S1). This suggests that the model can be sufficiently calibrated using just one season of data in which a large range of ice cover values is observed.

10.1029/2025GL120498

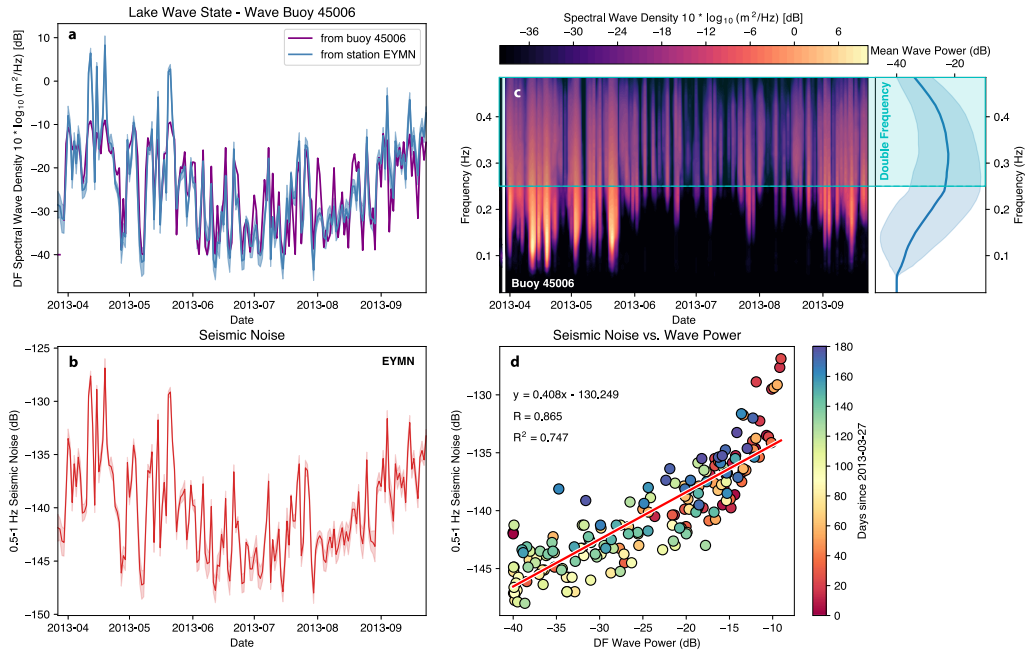

Figure 5. Using station EYMN to estimate the spectral wave density observed at buoy 45006 from 27 March to 23 September 2013. (a) Double-frequency spectral wave density with buoy measurements shown in purple and 0.5–1 Hz seismic noise in blue. (b) Daily seismic power spectral density within the 0.5–1 Hz band at station EYMN used for the prediction in panel (a). (c) Spectrogram of spectral wave density measured by buoy 45006. The mean spectral wave density is shown to the right. The blue box shows the double-frequency portion of the spectrum (0.25–0.5 Hz) used for the estimates in panel (a). (d) Linear fit between seismic noise in the lake microseism band (0.5–1 Hz) and the double-frequency wave power (0.25–0.5 Hz) used for predictions in panel (a).

3.3. Comparison to Wave Buoy Data

Although we find reasonably strong daily correlation between 0.5–2 Hz seismic noise and ice cover, approximately 40% of the daily seismic noise remains unexplained by changes in ice cover alone. We hypothesize that this unexplained data residual is due to fluctuations in lake wave state, which are less strong in the yearly averaged correlations due to the averaging procedure (e.g., only ∼15% of data variance remains unexplained in the yearly correlations). Unfortunately, wave buoys on the Great Lakes are deployed only during ice-free conditions, so we cannot directly test this hypothesis.

To explore the impact of lake wave state on seismic noise observed at EYMN and to evaluate the double-frequency microseism hypothesis, we turn to lake buoy data. Wave buoy 45006 provides information about potential sources of microseismic noise via spectral wave density (Figure 5). It reliably records swell frequencies only up to 0.5 Hz, meaning that we can investigate the double-frequency mechanism only up to 1 Hz. We therefore investigate seismic frequencies within the 0.5–1 Hz band.

The correlation between 0.5–1 Hz daily seismic noise and 0.25–0.5 Hz spectral wave power during ice-free periods is strong, with a correlation coefficient $R = 0.87$ (∼75% variance explained). This is consistent with expectations of the double-frequency mechanism of secondary microseism generation (Ardhuin et al., 2012; Hasselmann, 1963; Longuet-Higgins, 1950). This also suggests that our daily predictions of ice cover could be improved (more variance explained) if lake-buoy measurements were available during semi-frozen periods to account for variations in wave state.

4. Discussion

We show that a simple linear model can be used to relate seismic noise in the lake-microseism band to lake ice cover with considerable accuracy. This is similar to previous observations of the impact of sea ice on short-period microseism by damping ocean waves (Chen et al., 2025; John & West, 2025b; Tsai & McNamara, 2011). Lake ice estimates at the yearly average timescale ($R^2 = 0.87$, Figure 3) are more accurate than at the daily timescale

($R^2 = 0.58$, Figure 4) likely because variations due to lake-swell state are more prominent in the daily data and tend to average out over the course of weeks or months. To better explain the seismic data at daily or hourly timescales would require a more complex model that also considers proxies for the microseismic source such as lake-wave speed, wind speed, wave height, or spectral wave density (Ardhuin et al., 2012; Chen et al., 2025). Determining such microseism source parameters accurately is challenging and would require either in situ wave buoy observations during partially frozen periods, which are nontrivial to install and maintain especially in difficult to access locations such as alpine or arctic, or detailed finite element modeling such as WAVEWATCH III modified to consider complex ice-wave interactions (Hu et al., 2025). Our approach considering ice cover in isolation of complex source characteristics is useful for its simplicity.

This study demonstrates that lake-averaged ice cover can be predicted with reasonable accuracy using just a single seismometer. An important simplification is that we approximate ice cover as a single lake-averaged value. In reality, ice distribution can vary spatially across the lake (Figure S7 in Supporting Information S1). By considering only the local lake ice cover near a seismometer (e.g., Chen et al., 2025; Tsai & McNamara, 2011), we could potentially increase daily correlations, improving daily ice cover predictions over a smaller section of the lake. In turn, variations in seismic amplitudes observed across networks of seismometers around the lake could be used to constrain the spatial variability of ice cover (John & West, 2025b; Tsai & McNamara, 2011), reducing uncertainties as well as susceptibility to spurious local noise sources not associated with the lake-generated microseism. This would allow for near real-time spatiotemporal monitoring of lake ice cover and lake wave state at daily or hourly timescales. This will be the topic of a future study.

Coefficients of the linear model contain information about the underlying physics, reflecting lake and coastline area/geometry, average lake wave state, station distance from lake shore, and crustal attenuation. As shown in Figures S2 and S3 in Supporting Information S1, different linear models are obtained for different station-lake pairings. Lake-microseism noise could therefore be used to infer physical properties of the crust and/or lake state if one or the other is known. Indeed, this presents both an opportunity and a challenge for future applications to estimate ice cover on lakes that are less well instrumented than the Great Lakes. We show that just one season of ice cover data estimated from satellite imagery is sufficient to empirically determine the coefficients of the model that represent these physical properties (Figure 4c and Figure S4 in Supporting Information S1). However, satellite-based estimates of ice cover are not routinely available for smaller lakes.

The study of lake-generated microseisms is still in its infancy, with only a handful of lakes studied to date including Yellowstone Lake (Farrell et al., 2023; Smalls et al., 2019), Great Slave Lake (Xu et al., 2017), the Great Lakes (Anthony et al., 2018), and Lake Malawi (Carchedi et al., 2022). Of these lakes, the microseism generation mechanism has been determined at only Yellowstone Lake, which is consistent with the double-frequency mechanism based on the lake-generated microseism occurring at approximately twice the peak swell frequency (Farrell et al., 2023; Smalls et al., 2019). Interference between incident and shoreline reflected waves (Class II, Ardhuin et al., 2011) is the likely cause (Farrell et al., 2023). At larger lakes, such as Lake Malawi, the generation mechanism(s) are more complex and multiple wind-wave source regions likely operate. Complex lake geometry, nearby topography, or variable wind systems impacting different areas of the lake may create their own evolving microseism sources (Carchedi et al., 2022).

The dominant mechanism for lake-generated microseism at the Great Lakes is debated. Anthony et al. (2018) showed that the peak swell frequencies (0.1–0.14 Hz) tend to be lower than expected for a double-frequency mechanism (Anthony et al., 2018). They also explored expected frequencies of amplification from resonance due to bathymetry (Longuet-Higgins, 1950; Tanimoto, 2013) and found that the amplified frequencies (~1.1 Hz) are too high to explain their microseism observations. Similarly, we find that the peak spectral wave density at wave buoy 45006 occurs at ~0.3 Hz (Figure 5c), while the peak lake-generated microseism observed at station EYMN occurs at ~1 Hz (Figure 2b). To test the hypothesis of the double-frequency mechanism, we take a different approach by exploring the ability of the half-frequency portion of the spectral wave density to explain our seismic observations and find a high correlation ($R = 0.87$), which supports the double-frequency mechanism for lake microseism generation in Lake Superior. However, the mismatch between the peak swell frequency and the observed lake-generated microseism peak does imply that the dominant swell energy is not directly coupled into Rayleigh wave energy at twice the frequency but is instead being amplified at higher frequencies. We suggest that this could be due to amplification of the secondary microseism due to bathymetry, which is predicted to occur at 1–3 Hz for western portion of Lake Superior (Anthony et al., 2018; Longuet-Higgins, 1950).

Amplification may act like a filter that, when convolved with the relatively broadband pressure forcing at the lake bottom caused by 0.2–0.4 Hz swell, produces a microseism that peaks at ∼1 Hz for Lake Superior.

5. Conclusions

We show that observations of the 0.5–2 Hz lake-generated microseism at stations located near the Great Lakes provide a simple and effective proxy for lake ice cover. Using 15 years of data at station EYMN, we find that yearly average power in the 0.5–2 Hz lake-microseism band during peak cold months linearly covaries with Lake Superior ice cover averaged during that same time, with a correlation of $R = -0.93$ (∼87% variance explained). Applied to the 2014 "Polar Vortex" season, the calibrated linear model reproduces daily ice cover with $R = -0.74$ (∼58% variance explained). The lower predictability of daily ice cover is likely due to unaccounted for daily variability in wave state, which should average out at longer timescales. Comparisons with wave buoy spectra during the unfrozen season show that 0.25–0.5 Hz wave power explains much of the 0.5–1 Hz seismic noise ($R = 0.87$), consistent with the double-frequency (secondary) microseism mechanism.

These results demonstrate that: (a) a data-driven, lake–station specific linear transfer function can translate seismic noise into accurate average ice-cover estimates, (b) one season spanning a wide range of ice conditions is sufficient to calibrate the model, and (c) part of the residual daily variability reflects contemporaneous lake-wave state not captured by ice cover alone. The method presented here offers a single-station, continuous approach for monitoring ice and wave conditions on lakes in remote areas where conventional observations are limited. It also provides a foundation for future efforts leveraging seismic networks to understand spatial variability in lake ice cover.

Conflict of Interest

The authors declare no conflicts of interest relevant to this study.

Data Availability Statement

Lake ice cover was obtained from https://coastwatch.glerl.noaa.gov/statistics/great-lakes-ice-concentration/ and https://www.glerl.noaa.gov/data/ice/#historical (last accessed on 19 February 2026). Wave buoy data was obtained from https://www.ndbc.noaa.gov/ (last accessed on 19 February 2026). Seismic spectra for network code US were obtained from the EarthScope Data Management Center's Modular Utility for Statistical Knowledge Gathering (MUSTANG) system https://service.earthscope.org/mustang/ (last accessed on 19 February 2026). The codes used in this study are available for download at https://github.com/jbrussell/MUSTANG-microseism-ice (last accessed on 19 February 2026) and are archived at Zenodo (Russell, 2026).

Acknowledgments
We thank Associate Editor Victor Tsai, reviewer Michael West, and an anonymous reviewer for their constructive feedback, which helped improve this manuscript. We thank the Syracuse University Earth and Environmental Sciences faculty listserv for helping spark initial ideas for this study. JR acknowledges support from NSF Award PHY-2308989.

References

Anthony, R. E., Ringler, A. T., & Wilson, D. C. (2018). The widespread influence of Great Lakes microseisms across the midwestern United States revealed by the 2014 polar vortex. *Geophysical Research Letters*, *45*(8), 3436–3444. https://doi.org/10.1002/2017GL076690

Anthony, R. E., Ringler, A. T., & Wilson, D. C. (2022). Seismic background noise levels across the Continental United States from USArray transportable array: The influence of geology and geography. *Bulletin of the Seismological Society of America*, *112*(2), 646–668. https://doi.org/10.1785/0120210176

Ardhuin, F., Balanche, A., Stutzmann, E., & Obrebski, M. (2012). From seismic noise to ocean wave parameters: General methods and validation. *Journal of Geophysical Research*, *117*(C5), 1–19. https://doi.org/10.1029/2011jc007449

Ardhuin, F., Gualtieri, L., & Stutzmann, E. (2015). How ocean waves rock the Earth: Two mechanisms explain microseisms with periods 3 to 300s. *Geophysical Research Letters*, *42*(3), 765–772. https://doi.org/10.1002/2014GL062782

Ardhuin, F., Stutzmann, E., Schimmel, M., & Mangeney, A. (2011). Ocean wave sources of seismic noise. *Journal of Geophysical Research*, *116*(June), 1–21. https://doi.org/10.1029/2011JC006952

Carchedi, C. J. W., Gaherty, J. B., Webb, S. C., & Shillington, D. J. (2022). Investigating short-period lake-generated microseisms using a broadband array of onshore and lake-bottom seismometers. *Seismological Research Letters*, *93*(3), 1585–1600. https://doi.org/10.1785/0220210155

Casey, R., Templeton, M. E., Sharer, G., Keyson, L., Weertman, B. R., & Ahern, T. (2018). Assuring the quality of IRIS data with MUSTANG. *Seismological Research Letters*, *89*(2A), 630–639. https://doi.org/10.1785/0220170191

Chen, J.-C. F., Park, S., & Macayeal, D. R. (2025). Tracking multiyear sea - Ice variation in the Arctic Ocean over decades with microseism. *Geophysical Research Letters*, *52*(2), e2024GL111159. https://doi.org/10.1029/2024GL111159

Farrell, J., Koper, K. D., & Sohn, R. A. (2023). The relationship between wind, waves, bathymetry, and microseisms in Yellowstone Lake, Yellowstone National Park. *Journal of Geophysical Research: Solid Earth*, *128*(7), 1–18. https://doi.org/10.1029/2022JB025943

Hasselmann, K. (1963). A statistical analysis of the generation of microseisms. *Reviews of Geophysics*, *1*(2), 177–210. https://doi.org/10.1029/RG001i002p00177

Hu, H., Titze, D., Fujisaki-Manome, A., Mroczka, B., Wang, J., Hawley, N., et al. (2025). Winter ice-wave modeling with WAVEWATCH III in Lake Erie. *Journal of Geophysical Research: Oceans*, *130*(1), e2024JC021146. https://doi.org/10.1029/2024JC021146

Imrit, M. A., & Sharma, S. (2021). Climate change is contributing to faster rates of Lake Ice loss in Lakes around the northern hemisphere. *Journal of Geophysical Research: Biogeosciences*, *126*(7), 1–13. https://doi.org/10.1029/2020JG006134

Janiszewski, H. A., Eilon, Z., Russell, J. B., Brunsvik, B., Gaherty, J. B., Mosher, S. G., et al. (2022). Broad-band ocean bottom seismometer noise properties. *Geophysical Journal International*, *233*(1), 297–315. https://doi.org/10.1093/gji/ggac450

John, S., & West, M. E. (2025a). Appropriateness of the McNamara and Bulland's (2004) methodology for computing frequency-dependent seismic power (pp. 1–8). Retrieved from http://arxiv.org/abs/2410.14071

John, S., & West, M. E. (2025b). Storms, sea ice, and microseismic noise in Alaska. *Journal of Geophysical Research: Solid Earth*, *130*(4), e2024JB030603. https://doi.org/10.1029/2024JB030603

Koper, K. D., & Hawley, V. L. (2010). Frequency dependent polarization analysis of ambient seismic noise recorded at a broadband seismometer in the central United States. *Earthquake Science*, *23*(5), 439–447. https://doi.org/10.1007/s11589-010-0743-5

Longuet-Higgins, M. S. (1950). A theory of the origin of microseisms. *Philosophical Transactions of the Royal Society of London*, *243*(1–35), 12–53. https://doi.org/10.1098/rsta.1950.0012

Maurer, J. M., Schaefer, J. M., Russell, J. B., Rupper, S., Wangdi, N., Putnam, A. E., & Young, N. (2020). Seismic observations, numerical modeling, and geomorphic analysis of a glacier lake outburst flood in the Himalayas. *Science Advances*, *6*(38), eaba3645. https://doi.org/10.1126/sciadv.aba3645

McNamara, D. E., & Buland, R. P. (2004). Ambiente noise levels in the continental United States. *Bulletin of the Seismological Society of America*, *94*(4), 1517–1527. https://doi.org/10.1785/012003001

Park, J., Vernon, F. L., & Lindberg, C. R. (1987). Frequency dependent polarization analysis of high-frequency seismograms. *Journal of Geophysical Research*, *92*(B12), 12664–12674. https://doi.org/10.1029/jb092ib12p12664

Russell, J. (2026). jbrussell/MUSTANG-microseism-ice (v1.0.0) [Software]. *Zenodo*. https://doi.org/10.5281/zenodo.18706056

Simard, B., Isaacs, D., Langis, G., Langlois, D., Weir, L., Desjardins, L., et al. (2005). *MANICE: Manual of standard procedures for observing and reporting ice conditions* (9th ed.). Canadian Ice Service.

Smalls, P. T., Sohn, R. A., & Collins, J. A. (2019). Lake-bottom seismograph observations of microseisms in Yellowstone Lake. *Seismological Research Letters*, *90*(3), 1200–1208. https://doi.org/10.1785/0220180242

Tanimoto, T. (2013). Excitation of microseisms: Views from the normal-mode approach. *Geophysical Journal International*, *194*(3), 1755–1759. https://doi.org/10.1093/gji/ggt185

Tsai, V. C., & McNamara, D. E. (2011). Quantifying the influence of sea ice on ocean microseism using observations from the Bering Sea, Alaska. *Geophysical Research Letters*, *38*(22), 1–5. https://doi.org/10.1029/2011GL049791

Wang, J., Xue, P., Pringle, W., Yang, Z., & Qian, Y. (2022). Impacts of lake surface temperature on the summer climate over the Great Lakes region. *Journal of Geophysical Research: Atmospheres*, *127*(11), 1–20. https://doi.org/10.1029/2021JD036231

Xu, Y., Koper, K. D., & Burlacu, R. (2017). Lakes as a source of short-period (0.5–2 s) microseisms. *Journal of Geophysical Research: Solid Earth*, *122*(10), 8241–8256. https://doi.org/10.1002/2017JB014808

Yang, T. Y., Kessler, J., Mason, L., Chu, P. Y., & Wang, J. (2020). A consistent Great Lakes ice cover digital data set for winters 1973–2019. *Scientific Data*, *7*(1), 1–12. https://doi.org/10.1038/s41597-020-00603-1